Electronic Control of Conformation in Mixed-Phosphine Complexes of the Ruthenium η^5-Indenyl Fragment

Eric J. Derrah,[†] Jazmin C. Marlinga,[†] Debbie Mitra,[‡] Dawn M. Friesen,[†]
Shaun A. Hall,[†] Robert McDonald,[§] and Lisa Rosenberg*,[†]

*Department of Chemistry, University of Victoria, P.O. Box 3065, Victoria, British Columbia,
Canada V8W 3V6, Department of Chemistry, University of Manitoba, Winnipeg, Manitoba,
Canada R3T 2N2, and X-ray Crystallography Laboratory, Department of Chemistry,
University of Alberta, Edmonton, Alberta, Canada T6G 2G2*

The solid-state conformations of a series of new, mixed secondary and tertiary phosphine complexes of the general formula [Ru(η^5-indenyl)Cl(PPh₃)(HPR₂)] have been shown to persist in solution, largely because of the electronic requirements of the ancillary η^5-indenyl ligand in these complexes. The crystallographically observed conformations, with the indenyl benzo ring lying anti to the secondary phosphine across the Ru−η^5-indenyl bond, were diagnosed in solution from chemical shift differences for PPh₃ signals in the low-temperature-limiting ^{1}H and ^{13}C NMR spectra. These conformations were tuned by varying the relative trans influences of the different piano-stool legs, in particular through preparation of the analogous hydrido complexes [Ru(η^5-indenyl)H(PPh₃)(HPR₂)], which resulted in structures with the indenyl benzo ring anti to the hydride ligand. These studies provide evidence for the reasonably strong trans influence of coordinated secondary phosphines relative to PPh₃. Implications for the ancillary ligand behavior of secondary phosphines are discussed.

Introduction

Transition-metal-mediated addition reactions of the P−H bonds of primary and secondary phosphines are rare yet may provide a general synthetic route to the regio- and/or stereocontrolled synthesis of phosphines not accessible by traditional acid-, base-, or radical-catalyzed hydrophosphination reactions.[1] Critical to the development of transition-metal-mediated hydrophosphination is a clear understanding of the ligand behavior of phosphines containing potentially reactive P−H bonds. The Lewis basicity of the substrate phosphines is a key issue, as is the extent to which their metal coordination impedes or encourages P−H activation. Meanwhile, given that many complexes containing coordinated primary or secondary phosphines do *not* exhibit spontaneous addition of the P−H bond, the general use of secondary phosphines as ancillary ligands in homogeneous catalysis is underexplored. In these contexts, we have been studying the substitution reactions of [Ru(η^5-indenyl)Cl(PPh₃)₂] (**1**) with secondary phosphines, HPR₂.

We chose to study the reactivity of **1** with secondary phosphines because of its well-established substitution chemistry and the high lability of this pseudooctahedral, prochiral complex. Complex **1** finds use as a catalyst and stoichiometric reagent for a range of C−C bond-forming reactions, frequently exhibiting higher activity in these reactions than its Cp or Cp* analogues,[2] a phenomenon referred to as the "indenyl effect". Such reactivity trends are typically attributed to relatively facile ring slippage of the η^5-indenyl ligand of an 18-electron complex to an η^3 form, freeing a coordination site and providing access to a low-energy associative substitution pathway (i.e. with rate dependence on the concentration of the incoming ligand).[3] However, several recent studies point to the importance of ground-state effects (i.e. the weakness of the η^5-indenyl-M interaction versus η^5-Cp−M interactions), along with or instead of transition state effects (i.e. facile hapticity change) on the relative rates of ligand substitution at indenyl and Cp complexes.[4] Thus, both η^5-indenyl *and* Cp metal interactions are strengthened by loss of a phosphine from these pseudooctahedral precursors, but a weakened indenyl−metal interaction in the ground state reduces the overall barrier to phosphine dissociation. Consistent with this alternative explanation for the "indenyl effect", kinetic studies of phosphine substitution reactions at complex **1** show that these reactions, which are orders of magnitude faster than reactions at the analogous η^5-Cp or Cp* complexes, proceed via a dissociative mechanism that does not require an indenyl hapticity change.[5] We describe here the synthesis and study of coordinatively saturated, mixed secondary/

---

* To whom correspondence should be addressed. Tel: 250-721-7173. Fax: 250-721-7147. E-mail: lisarose@uvic.ca.
† University of Victoria.
‡ University of Manitoba.
§ University of Alberta.
(1) (a) Wicht, D. K.; Kourkine, I. V.; Lew, B. M.; Mulei Nthenge, J.; Glueck, D. S. *J. Am. Chem. Soc.* **1997**, *119*, 5039. (b) Douglass, M. R.; Marks, T. J. *J. Am. Chem. Soc.* **2000**, *122*, 1824.

(2) (a) Cadierno, V.; Diez, J.; Gamasa, M. P.; Gimeno, J.; Lastra, E. *Coord. Chem. Rev.* **1999**, *193−195*, 147. (b) Trost, B. M.; Toste, F. D.; Pinkerton, A. B. *Chem. Rev.* **2001**, *101*, 2067.
(3) Crabtree, R. H. *The Organometallic Chemistry of the Transition Metals,* 3rd ed.; Wiley-Interscience: New York, 2001; p 101.
(4) (a) Kubas, G. J.; Kiss, G.; Hoff, C. D. *Organometallics* **1991**, *10*, 2870. (b) Calhorda, M. J.; Romão, C. C.; Veiros, L. F. *Chem. Eur. J.* **2002**, *8*, 868.

tertiary phosphine complexes in which the P–H groups are inert toward oxidative addition. These systems clearly demonstrate the strong trans influence of secondary phosphines, relative to PPh$_3$, and the impact this can have on geometric isomerism and reactivity in these complexes.
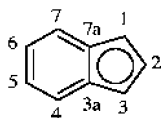
Results and Discussion

Mixed-phosphine complexes **2a,b** result from the addition of dicyclohexyl- or diphenylphosphine to complex **1**, with displacement of one PPh$_3$ ligand (Scheme 1, top). ^{31}P{^{1}H} NMR spectra are diagnostic of the structures shown, consisting of two doublets ($^2J_{PP} \approx 45$ Hz), one of which shows further splitting of $^1J_{H-P} \approx$ 350–375 Hz in the corresponding, proton-coupled ^{31}P NMR spectra. Also diagnostic of the coordinated secondary phosphines in these complexes are doublets of multiplets, corresponding to the secondary phosphine P–H groups, in the ^{1}H NMR spectra of **2a,b**, at 4.05 ppm (dt, $^1J_{PH} \approx 354$ Hz, $^3J_{HH} = 4.2$ Hz, $^3J_{PH}$ not resolved) for R = Cy and 6.35 ppm (dd, $^1J_{PH} \approx 375$ Hz,

Scheme 1
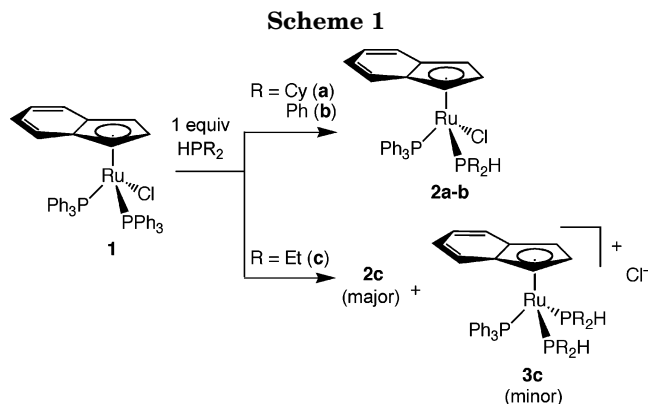
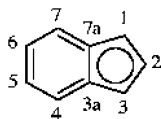$^3J_{PH} = 2.6$ Hz) for R = Ph. The ^{1}H and ^{13}C{^{1}H} spectra of **2a,b** are complicated, relative to those of **1**, by the lack of a plane of symmetry at ruthenium in these complexes, which renders diastereotopic the halves of the planar-bound indenyl ring, as well as the two secondary phosphine R groups, (see Tables 1 and 2 for ^{1}H and ^{13}C{^{1}H} NMR spectroscopic data).

Table 1. 500 MHz ^{1}H NMR Data for Complexes 2a–c and 3c in CDCl$_3$ and 5a,b in C$_6$D$_6$ at 300 K^a

	H$_7$, H$_4$	H$_6$, H$_5$	H$_2$	H$_3$, H$_1$	PPh$_3$	other
2a	7.49 (d, 1H, 8.4) 6.47 (d, 1H, 8.3)	7.44 (dt, 1H, 7.5, 1.5) 6.93 (t, 1H, 7.5)	5.01 (dt, 1H, 4.0, 2.7)	4.70–4.69 (m, 1H) 3.51 (br s, 1H, 4)	H$_m$, H$_p$ 7.28, 7.24 (o br s, 9H, 30, 22) H$_o$ 7.07 (br s, 6H, 160)	H–PCy$_2$: 4.05 (dt, 1H, 354, 4.2) Cy (HPCy$_2$): 2.25–2.18 (m, 1H), 1.92–1.87 (o br m, 2H), 1.86-1.72 (o br m, 4H), H$_g$ 1.65–1.61 (br m, 2H), 1.60–1.51 (o m, 3H), 1.49–1.40 (m, 1H), 1.39–1.09 (o m, 7H), 0.92–0.83 (o m, 2H)
2b	7.54 (d, 1H, 8.4) 6.37 (d, 1H, 8.5)	7.39 (t, 1H, 7.5) 6.91 (t, 1H, 7.5)	5.12 (br s, 1H, 10)	4.94 (br s, 1H, 8) 3.51 (s, 1H)	H$_p$ (overlaps HPPh$_2$) 7.31–7.25 (o m, 3H) H$_m$ 7.16 (dt, 6H, 7.8, 1.9) H$_o$ 6.90–6.70 (br s, 6H, 40)	H$_o$ (HPPh$_2$) 7.64-7.60 (m, 2H); H$_m$, H$_p$ (HPPh$_2$, overlaps PPh$_3$) 7.3–-7.25 (o m, 6H); H$_o$, H$_m$ (HPPh$_2$) 6.86–6.82 (m, 2H) H–PPh$_2$: 6.35 (dd, 375, 2.6)
2c	7.51 (d, 1H, 8.4) 6.62 (d, 1H, 8.3)	7.34 (t, 1H, 7.4)	4.97 (q or dd, 1H, 2.7)	4.79–4.78 (m, 1H) 3.71 (br s, 1H, 6)	H$_m$, H$_p$ 7.32–7.24 (o m, 9H) H$_o$ 7.11 (t, 6H, 8.6)	H–PEt$_2$: 4.05 (dm, 1H, 352) Et: PCH$_2$ (A) 2.01–1.92 (m, 1H); PCH$_2$ (A′) 1.93–1.83 (m, 1H); PCH$_2$ (B) 1.82–1.72 (m, 1H); PCH$_2$ (B′) 1.55–1.45 (m, 1H); CH$_3$ (A) 1.04 (dt, 3H, 7.7, 15.7); CH$_3$ (B) 0.98 (dt, 3H, 7.7, 15.6)
3c	7.18–7.15 (m, 2H)	6.87–6.83 (m, 2H)	5.71 (2, 1H)	5.22 (d, 2H, 2.5)	H$_p$ 7.43–7.41 (m, 3H) H$_m$ 7.38–7.34 (m, 6H) H$_o$ 6.73 (br t, 6H, 9.0)	H–PEt$_2$: 3.93 (dm, 1H, 342) Et: PCH$_2$ (A) 1.94–1.85 (m, 2H); PCH$_2$ (B, B′, A′) 1.76–1.63 (o m, 6H); CH$_3$ (A) 1.12 (dt, 6H, 7.8, 16.0); CH$_3$ (B) 0.91 (dt, 6H, 7.7, 16.8)
5a	7.26 (d, 1H, 8.0) 6.32 (d, 1H, 8.5)	6.95 (t, 1H, 7.5) 6.82 (t, 1H, 7.3)	5.7 (s, 1H)	5.29 (s, 1H) 4.74 (s, 1H)	H$_o$ 7.47–7.43 (o m, 6H) H$_m$ 7.08–7.05 (o m, 6H) H$_p$ 7.03–7.00 (o m, 3H)	H–PCy$_2$: 3.49 (ddd, 1H, 315.1, 5.5) Cy: 1.82–1.52 (o m, 11H), 1.39–1.25 (o m, 5H), 1.20-0.98 (o m, 3H), 0.88–0.75 (o m, 2H), 0.66–0.56 (o m, 1H) Ru–H: −16.57 (t, 1H, 32.5)
5b	6.42 (d, 1H, 8.0) 6.23 (d, 1H, 8.0)	6.82–6.76 (o m, 2H)	5.88 (s, 1H)	4.91 (s, 1H) 4.69 (s, 1H)	H$_o$ 7.24–7.20 (m, 6H) H$_m$, H$_p$ PPh$_3$ HPPh$_2$ 7.10–6.93 (o m, 16H)	H–PPh$_2$: 5.85 (dd, 335.6, 11.0) Ph: H$_o$ 7.81–7.77 (m, 2H) Ru–H: −15.14 (dd, 1H, 30.0, 30.5)

^{a} δ in ppm (multiplicity, relative intensity, and J_{avg} or $\omega_{1/2}$ in Hz are given in parentheses), o = overlapping.

Table 2. 125 MHz ^{13}C{^{1}H} NMR Data for the η^5-Indenyl (C$_9$H$_7$) and Other Ligands for Complexes 2a−c and 3c in CDCl$_3$ and 5a,b in C$_6$D$_6$ at 300 K^a

|	η^5-C$_9$H$_7$						PPh$_3$	others
	C$_6$, C$_5$	C$_7$, C$_4$	C$_{3a}$, C$_{7a}$	$\Delta\delta$(C$_{3a,7a}$)^b	C$_2$	C$_3$, C$_1$		
2a	126.8 (s) 126.2 (s)	124.4 (s) 123.6 (s)	110.6 (d, 4) 108.2 (d, 3)	−21.3 (av)	83.4 (d, 11)	64.8 (d, 11) 61.6 (s)	C$_{ipso}$ (br, in baseline) C$_{ortho}$ 134 (br s, 126) C$_{para}$ 129.1 (s) C$_{meta}$ 127.4 (d, 9)	HPCy$_2$: PCH 41.6 (d, 27), 37.3 (dd, 24.3) others 33.5 (d, 7), 32.8 (d, 4) 32.4 (s), 28.1 (s), 27.6 (d, 11.7), 27.5-27.4 (three o), 26.6 (d, 4)
2b	127.1 (s) 126.6 (s)	124.5 (s) 123.8 (s)	111.1 (d, 3) 108.5 (d, 4)	-20.9 (av)	87.4 (s)	68.0 (d, 10) 62.5 (s)	C$_{ortho}$ 133.9 (br s, 42) C$_{para}$ 129.1 (s) C$_{meta}$ 127.5 (d, 10)	HPPh$_2$: C$_{ipso}$ 134.4 (dd, 43, 4), 134.0 (d, 49), C$_{ortho}$ 132.8 (d, 9), 132.3 (d, 10) C$_{para}$ 129.9 (d, 1), 129.4 (d, 2) C$_{meta}$ 128.4 (d, 9), 127.9 (d, 10)
2c	126.8 (s) 126.3 (s)	124.3 (s) 124.3 (s)	110.7 (d, 4) 108.3 (s)	−21.2 (av)	86.2 (d, 9)	64.2 (d, 9) 63.8 (s)	C$_{ipso}$ 136.0 (d, 42) C$_{ortho}$ 134.0 (d, 11) C$_{para}$ 129.4 (d, 1) C$_{meta}$ 127.8 (d, 9)	HPEt$_2$: PCH$_2$ (B) 19.2 (d, 29); PCH$_2$(A) 17.4 (dd, 28, 2); CH$_3$(A) 11.7 (d, 6); CH$_3$(B) 11.2 (d, 5)
3c	124.5 (s)	127.5 (s)	109.3 (s)	−21.4	92.0 (s)	70.8 (s)	C$_{ipso}$ 134.1 (d, 41) C$_{ortho}$ 133.0 (d, 10) C$_{para}$ 131.0 (d, 2) C$_{meta}$ 128.8 (d, 10)	HPEt$_2$: PCH$_2$(B) 20.2 (t, 16); PCH$_2$(A) 19.9 (t, 15); CH$_3$(A) 13.3 (t, 4); CH$_3$(B) 12.2 (t, 4)
5a	122.8 or 122.7 (o s) 121.9 (s)	122.8 or 122.7 (o s) 122.4 (s)	109.8 (s) 108.5	−21.6 (av)	85.7 (s)	71.1 (t, 8) 65.8 (t, 9)	C$_{ipso}$ 141.0 (d, 38) C$_{ortho}$ 135.5 (d, 9) C$_{para}$ 128.9 (s) C$_{meta}$ 127.8 (d, 9)	HPCy$_2$: PCH 38.2 (d, 21), 34.5 (dd, 38, 4), 28.1 (d, 11), 27.9−27.6 (o signals), 27.1 (d, 5)
5b	121.1 (s) 121.5 (o m)	123.3 (s) 121.5 (o m)	11.04 (s) 106.8	−22.1 (av)	87.8 (s)	71.1 (t, 10) 70.0 (t, 9)	C$_{ipso}$ 140.4 (dd, 41.2) C$_{ortho}$ 134.3 (br s) C$_{para}$ 129.1 (s) C$_{meta}$ 127.9 (s)	HPPh$_2$: C$_{ipso}$ 141.5 (d, 39), 139.4 (d, 44) C$_{ortho}$ 135.1 (br s) C$_{para}$ 129.6 (s) C$_{meta}$ 132.0 (d, 10)

^{a} δ in ppm (multiplicity and J_{PC} or $\omega_{1/2}$ in Hz are given in parentheses), o = overlapping. ^{b} $\Delta\delta$(C$_{3a,7a}$) = δ(C$_{3a,7a}$(η-indenyl complex)) − δ(C$_{3a,7a}$(η-sodium indenyl)); δ(C$_{3a,7a}$) for sodium indenyl 130.7 ppm.[5]

As shown at the bottom of Scheme 1, attempts to prepare the analogous diethylphosphine complex **2c** inevitably gave a mixture of the desired product and a cationic bis(diethylphosphine) complex, **3c**, resulting from the displacement of the chloride ion from **2c** by a second equivalent of diethylphosphine. Significant amounts of **3c** (up to 10%) formed even with carefully controlled addition of only 1 equiv of diethylphosphine to **1**.[6] As shown at the bottom of Scheme 2, addition of

$\geq$3 equiv of diethylphosphine to **1** gave complex **3c** as the major product, with up to 10−30% of **2c** and an impurity with solubility comparable to that of **3c**, which is probably the tris(phosphine) cation [Ru(η^5-indenyl)-(HPEt$_2$)$_3$]Cl (**4c**). Reaction of $\geq$3 equiv of diphenyl- or dicyclohexylphosphine with **1** in refluxing toluene yields

(5) Gamasa, M. P.; Gimeno, J.; Gonzalez-Bernardo, C.; Martin-Vaca, B. M. *Organometallics* **1996**, *15*, 302.

(6) The progress of the reaction of **1** with a deficiency of HPEt$_2$ (0.4 equiv), monitored by ^{31}P{^{1}H} NMR spectroscopy, indicates that substitution at **1** to yield **2c** dominates the reaction profile and is clearly much faster than substitution at **2c** to yield **3c**. However, under optimum conditions for isolation of **2c**, this kinetic distribution is skewed by the lower solubility of **3c**.
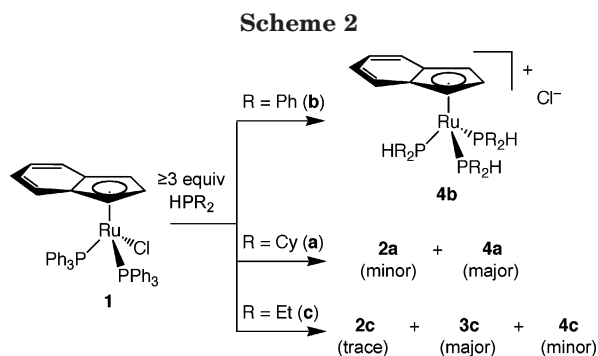
Scheme 2

the tris(secondary phosphine) cations **4a,b** as bright yellow precipitates (Scheme 2, top half), although the tris(dicyclohexylphosphine) complex **4a** was inevitably contaminated by the monosubstituted intermediate **2a**.[7] We have spectroscopically characterized the bis(diphenylphosphine) cation **3b**, which tends to coprecipitate with second crops of **2b** when the mixtures are allowed to stand for several weeks,[8] but have not observed the analogous bis(dicyclohexylphosphine) cation **3a**, even when reactions of **1** with 2−3 equiv of this phosphine were monitored by $^{31}P\{^{1}H\}$ NMR spectroscopy.

We obtained single crystals of **2a,b** suitable for X-ray diffraction analysis. The resulting molecular structures are shown in Figures 1 and 2, and selected bond distances and angles are listed in Table 3. The geometry at Ru in these three-legged piano-stool complexes is pseudooctahedral, with bond angles similar to those observed for a range of other neutral complexes of the formula "[Ru(indenyl)(X)(PPh₃)(L)]", although the PPh₃−Ru−L (L = secondary phosphine) angles are slightly compressed and appear at the low end of this range of values (93.9−104.3°).[9] The slip factors, Δ = 0.14 Å (**2a**) and 0.16 (**2b**), are consistent with η^5 coordination of the indenyl ligand showing only a slight distortion toward η^3 coordination (as "real" η^3 coordination slip factors fall in the range Δ = 0.69−0.80 Å).[10] The distances between Ru and the centroid of the η^5-indenyl ring (Ru−C*) in **2a,b**, 1.88 and 1.90 Å, respectively, are also typical of ruthenium indenyl complexes, and the Ru−P bond
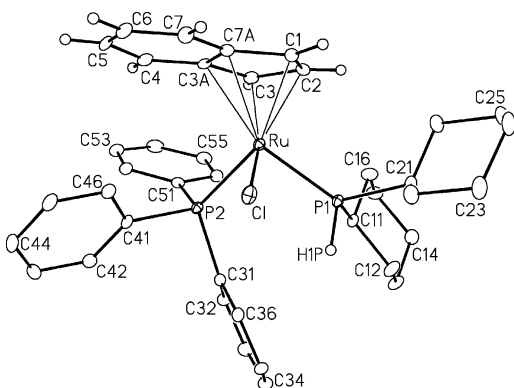

Figure 1. Perspective view of [RuCl(η^5-indenyl)(PPh₃)-(HPCy₂)] (**2a**) showing the atom-labeling scheme. Nonhydrogen atoms in this and subsequent figures are represented by Gaussian ellipsoids at the 20% probability level. Hydrogen atoms, when shown, are represented with arbitrarily small thermal parameters; phosphine phenyl and cyclohexyl hydrogens are not shown.
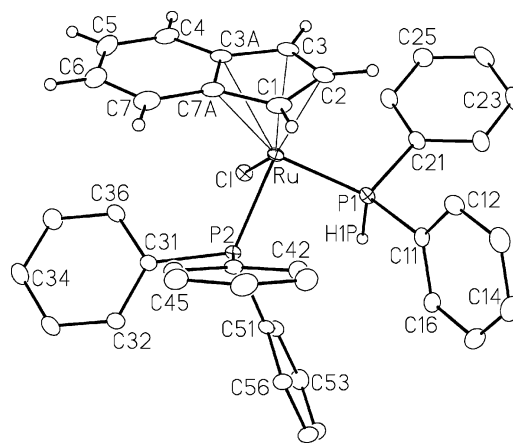

Figure 2. View of [RuCl(η^5-indenyl)(HPPh₂)(PPh₃)] (**2b**).

Table 3. Selected Interatomic Distances (Å) and Bond and Torsional Angles (deg) in the Structures of [RuCl(η^5-indenyl)(HPCy₂)(PPh₃)] (2a) and [RuCl(η^5-indenyl)(HPPh₂)(PPh₃)] (2b)

	2a	2b
Interatomic Distances		
Ru−P1	2.2642(10)	2.2307(9)
Ru−P2	2.3099(9)	2.3063(8)
Ru−Cl	2.4446(9)	2.4427(8)
Ru−C*[a]	1.883	1.902
Ru−C7A	2.330(4)	2.355(3)
Ru−C1	2.209(4)	2.161(3)
Ru−C2	2.158(4)	2.166(3)
Ru−C3	2.173(4)	2.229(3)
Ru−C3A	2.334(3)	2.357(3)
P1−H1P	1.23(4)	1.31(3)
Δ[b]	0.14	0.16
Bond Angles		
C*−Ru−P1[a]	126.2.	124.7
C*−Ru−P2[a]	123.5	124.3
C*−Ru−Cl[a]	124.0	125.6
P1−Ru−P2	94.75(3)	93.94(3)
P1−Ru−Cl	86.25(3)	86.35(3)
P2−Ru−Cl	91.71(3)	91.28(3)
fold angle (FA)[c]	6.7(5)	8.78(18)
hinge angle (HA)[d]	5.1(6)	6.63(18)
Torsional Angles		
C**−C*−Ru−P1[a,e]	172.6	173.2
C**−C*−Ru−P2[a,e]	−60.0	−61.8
C**−C*−Ru−Cl[a,e]	59.3	59.6

[a] C* = C7A−C1−C2−C3−C3A centroid. [b] Δ slip distortion parameter = d(Ru−C7A,C3A) − d(Ru−C1,C3). [c] Fold angle = angle between normals to planes defined by C1−C2−C3 and C7A−C3A−C4−C5−C6−C7. [d] Hinge angle = angle between normals to planes defined by C1−C2−C3 and C7A−C1−C3−C3A. [e] C** = C7A−C3A−C4−C5−C6−C7 centroid.

lengths of 2.2307(9)−2.3099(9) Å are within the normal range for ruthenium phosphine complexes (2.20−2.43

(7) The synthesis and characterization of **4b** was reported in: Westmore, J. B.; Rosenberg, L.; Hooper, T. S.; Willett, G. D.; Fisher, K. J. *Organometallics* **2002**, *21*, 5688.

(8) NMR data for [Ru(η^5-indenyl)(HPPh₂)₂(PPh₃)]Cl (**3b**), from analysis of a mixture of **2b** and **3b**: $^{31}P\{^{1}H\}$ (145.78 MHz, C₆D₆, δ) 49.5 (t, $^2J_{P-P}$ = 33 Hz, 1P, PPh₃), 39.0 (br d, 2P, HPPh₂); ^1H (360.14 MHz, C₆D₆, δ) 7.82−7.76 (m, 2H, H₀ PPh₂), 7.61−7.55 (m, 2H, H₀ PPh₂), 7.31−6.88 (overlapping m, remaining aromatic H and P*H*Ph₂ for **3b**, overlapping with aromatic signals due to **2b**), 6.76−6.73 (m, 2H, H₇/₄), 6.42 (br s, $\omega_{1/2}$ ≈ 5.5 Hz, 2H, H₁/₃), 6.19−6.16 (m, 2H, H₆/₅), 4.28 (br s, $\omega_{1/2}$ ≈ 5.2 Hz, 1H, H₂).

(9) See for example: (a) Kamigaito, M.; Watanabe, Y.; Ando, T.; Sawamoto, M. *J. Am. Chem. Soc.* **2002**, *124*, 9994. (b) Cadierno, V.; Conejero, S.; Gamasa, M. P.; Gimeno, J. *Organometallics* **2001**, *20*, 3175. (c) Cadierno, V.; Conejero, S.; Gamasa, M. P.; Gimeno, J. *Organometallics* **1999**, *18*, 582. (d) Sato, M.; Iwai, A.; Watanabe, M. *Organometallics* **1999**, *18*, 3208.
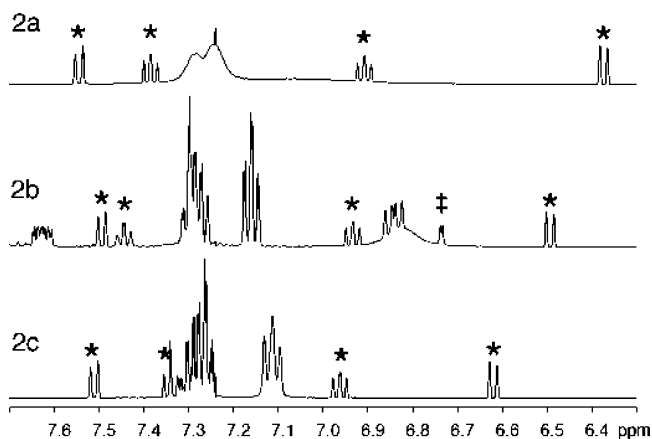
Figure 3. Aromatic region of 500 MHz ^{1}H NMR spectra for complexes **2a**−**c** in CDCl$_3$ at room temperature. Peaks due to H4−7 on the η^5-indenyl ligand are marked with asterisks (*), and the double dagger (‡) indicates half of the P−H signal in **2b**.

Å).[11] We examined the structures carefully for any unusual distances or angles involving the secondary phosphine P−H groups (these hydrogens were located and freely refined), since we observed broadening in the aromatic regions of room-temperature ^{1}H and ^{13}C{^{1}H} NMR spectra of these complexes (vide infra) (Figure 3 shows the aromatic region of ^{1}H NMR spectra for all three complexes **2a**−**c**.) A relatively high barrier to Ru−PPh$_3$ rotation in **2a,b** might indicate some bonding interaction between the coordinated P−H and Ru−Cl, which would force the R groups of the coordinated secondary phosphine toward the PPh$_3$ ligand, obstructing its free rotation. This type of intramolecular M−Cl···H−P interaction has not previously been observed for secondary phosphine complexes of transition metals, though examples do exist of phosphonium ions that form P$^+$−H···Hal$^-$ hydrogen bonds with their counterions in the solid state.[12] However, in both complexes, the Ru−Cl and P−H bond distances are normal, and Cl···H separations not less than 3 Å imply no unusual interactions. The IR spectra of **2a,b** are consistent with the solid-state structures: ν_{PH} stretches fall in the normal range of 2200−2300 cm^{-1} for secondary phosphines and are reasonably sharp, suggesting that no unusual H bonding is occurring in these complexes.[13]

As mentioned above, room-temperature ^{1}H and ^{13}C{^{1}H} NMR spectra of **2a,b** show broadening of some peaks in the aryl region, indicative of a dynamic process involving phenyl groups that is slow on the NMR time

scale(s). This broadening does not occur for **2c** (Figure 3), which contains the much smaller HPEt$_2$ ligand.[14] Variable-temperature NMR studies showed that this line broadening arises from slowed rotation around the Ru−PPh$_3$ bond in both complexes, which renders all three phenyl groups inequivalent at the low-temperature limit. This phenyl group exchange is most clearly illustrated by ^{13}C NMR spectra recorded for the HPCy$_2$ complex **2a** in CDCl$_3$ at variable, low temperatures. The aryl region of the room-temperature ^{13}C{^{1}H} NMR spectrum of **2a** (Figure 4a) shows a very broad signal at ∼134 ppm corresponding to C$_{ortho}$ and a slightly broadened singlet (129.1 ppm, C$_{para}$) and doublet (127.4 ppm, C$_{meta}$). A broadened C$_{ipso}$ signal is lost in the baseline slightly downfield from the signal at 134 ppm. Sharp, well-resolved signals for the indenyl benzo carbons (C4−7) are also found in this region; they remain sharp at all temperatures visited. Decoalescence of the phenyl signals occurs as the sample is cooled. Resolved peaks in the aryl regions of the low-temperature limiting spectra (at 210 K) of **2a** (Figure 4b) indicate the presence of three magnetically distinct phenyl groups. Line shape analysis of the ortho, meta, para, and ipso ^{13}C signals at various temperatures between 302 and 210 K gave self-consistent rate constants for this three-site exchange for **2a**, which allowed calculation of a barrier to rotation of $E_a \approx 9$ kcal/mol. As shown in Figure 3, the slowing of this exchange is also evident in ^{1}H spectra of the diphenylphosphine complex **2b**, and variable-temperature NMR studies of **2b** indicate that this complex has an analogous, low-symmetry ground-state solution structure, consistent with hindered rotation around the Ru−PPh$_3$ bond, although assignments were complicated by the presence of extra aryl signals due to the HPPh$_2$ ligand.

Although the three-legged piano stool structures of **2a,b** show no unusual bond lengths or angles, a feature common to both structures is the conformation of the η^5-indenyl group with respect to the three other ligands in the complexes. The benzo ring of the indenyl ligand lies opposite, or anti, to the HPR$_2$ ligand, across the C$_5$−Ru bond.

2a: R = Cy
2b: R = Ph
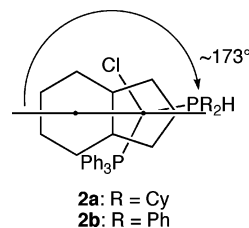
This places the indenyl arene ring very close to the triphenylphosphine, despite the considerable bulk of this ligand (see torsional angles in Table 3). If this conformation is also preferred for these molecules in solution, ring current shielding effects should give rise to large downfield chemical shifts for signals in the ^{1}H and ^{13}C{^{1}H} NMR spectra due to the phenyl group closest to the indenyl benzo ring. This can be seen clearly in the low-temperature-limiting spectra for **2a,b** (shown for complex **2a** in Figure 4). It is the resulting

(10) As shown in Table 3, hinge angles (HA) of less than 10° are also consistent with η^5 structures.[2a]

(11) Keisham, S. S.; Mozharivskyj, Y. A.; Carroll, P. J.; Rao Kollipara, M. *J. Organomet. Chem.* **2004**, *689*, 1249.

(12) Desiraju, G. R.; Steiner, T., *The Weak Hydrogen Bond in Structural Chemistry and Biology*; Oxford University Press: Oxford, U.K., 1999; p 269.

(13) In the absence of data for structurally similar examples of secondary phosphine complexes for which an *absence* of P−H hydrogen bonding is certain, it is difficult to predict the magnitude of the anticipated shift for ν_{PH} of these putative hydrogen-bonded P−H linkages. One report of hydrogen bonding for a series of (RO)$_2$PH(O) compounds, however, describes ν_{PH} shifts of 14 cm^{-1} to lower frequency as "significant": Corbridge, D. E. C. In *Topics in Phosphorus Chemistry*; Grayson, M., Griffiths, E. J., Eds.; Interscience: Toronto, 1969; Vol. 6, p 254.

(14) Ligand (cone angle): PPh$_3$ (145°), HPCy$_2$ (142.3°), HPPh$_2$ (125.7°), HPEt$_2$ (117°). Tolman, C. A. *Chem. Rev.* **1977**, *77*, 313.
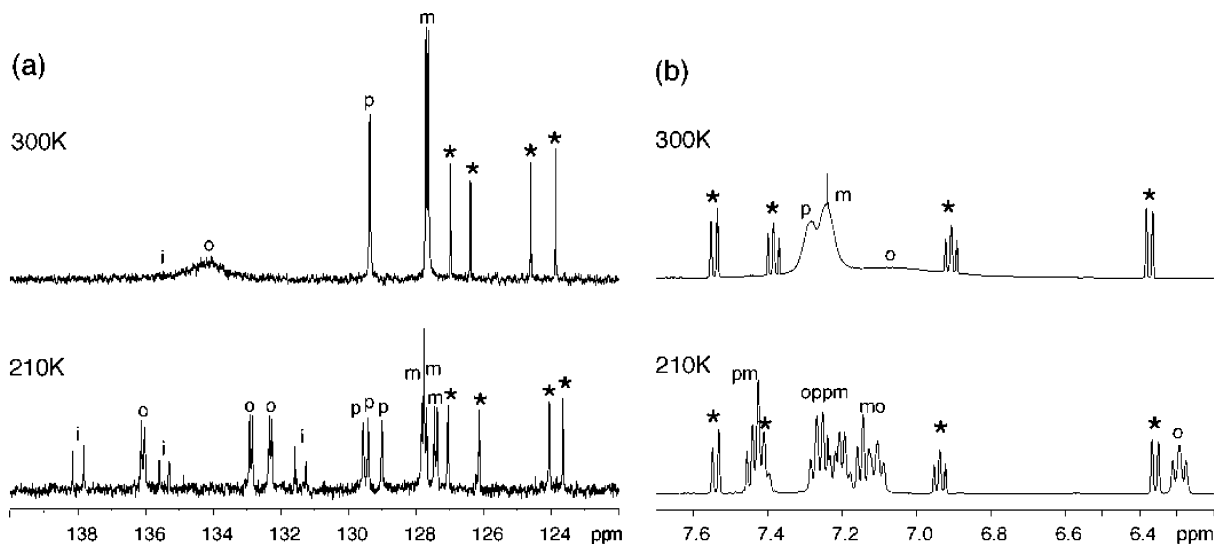
Figure 4. Aromatic region of variable-temperature (a) 125.7 MHz $^{13}C\{^{1}H\}$ and (b) 500 MHz ^{1}H NMR spectra for complex **2a** in CDCl$_3$. Peaks due to the benzo ring of the η^5-indenyl ligand are marked with asterisks (*), and aromatic peaks are labeled "i" (ipso), "o" (ortho), "m" (meta), and "p" (para). (See the Supporting Information for details of these assignments.)

large difference in chemical shifts for the three PPh$_3$ phenyl groups that causes the extreme broadening of peaks in the room-temperature NMR spectra of **2a,b**, since the coalescence temperature is raised relative to structures where the three Ph sites are less magnetically distinct. However, there is no doubt that the Ru–PPh$_3$ bond rotation is slowed in these complexes due to a degree of steric crowding, since the analogous complex of the smaller secondary phosphine HPEt$_2$ (**2c**) shows no broadening of peaks in its room-temperature spectrum (Figure 3).

That the (presumably freely rotating) indenyl ring shows a preferred solution conformation similar to the structures shown in Figures 1 and 2 is consistent with a proposal by Faller and Crabtree stating that the benzo ring of an η^5 indenyl ligand will tend to orient itself anti, across the C$_5$-centroid–Ru bond, to the highest trans-influence ligand in this piano-stool structure.[15] This takes into account the fact that, despite its η^5 coordination, the C$_5$ portion of the indenyl ligand in these complexes is best viewed as the pairing of an η^3-allyl and an η^2-"ene" fragment. The driving force for this conformational preference is (at least partial) aromatization of the indenyl benzo ring, effectively rendering the "ene" portion of the C$_5$ ring a very poor donor. The observed conformation of complexes **2a,b** implies that the secondary phosphines HPCy$_2$ and HPPh$_2$, which lie approximately anti to the indenyl benzo ring across the C$_5$–Ru bond, are stronger trans-influence ligands than either PPh$_3$ or Cl$^-$. For HPPh$_2$ relative to PPh$_3$ this is most easily explained by the increased donor strength of the secondary phosphine with replacement of an electron-withdrawing Ph group by a donating H group, while for HPCy$_2$, the presence of two strongly donating Cy groups and an H substituent should also provide stronger σ-donor ability.

To test the above explanation for a solution conformational preference of the η^5-indenyl ring in **2a,b**, and the resulting chemical shielding effects, we prepared the

(15) Faller, J. W.; Crabtree, R. H.; Habib, A. *Organometallics* **1985**, *4*, 929.

hydrido derivatives **5a,b**, as shown in eq 1.[16] X-ray

$$(1)$$
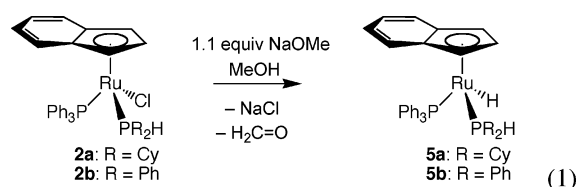
diffraction studies of single crystals of **5a,b** indicate that both complexes adopt a solid-state conformation placing the benzo ring of the η^5-indenyl ligand approximately anti to the very strongly trans-influencing hydride ligand (molecular structures are shown in Figures 5 and 6 and relevant bond distances and angles in Table 4). The hydride and PH ligands were located and freely refined in both structures, which display pseudo-octahedral geometries at Ru and normal bond distances and angles as described above for complexes **2a,b**. For complex **5a**, this moves the PPh$_3$ phenyl groups to a position well outside the influence of the C$_6$ indenyl ring, and accordingly, the room-temperature ^1H spectrum of this complex does not show the broadening of aryl peaks we observed in the spectra of **2a**, consistent with a
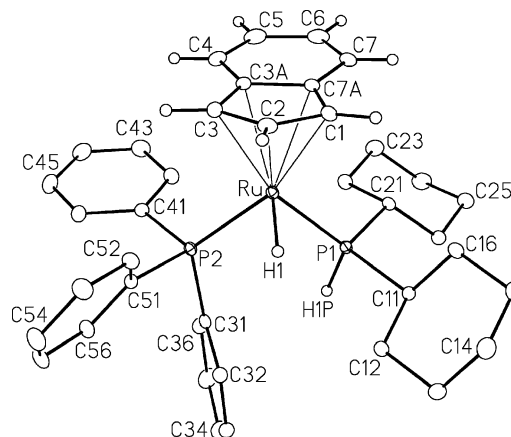

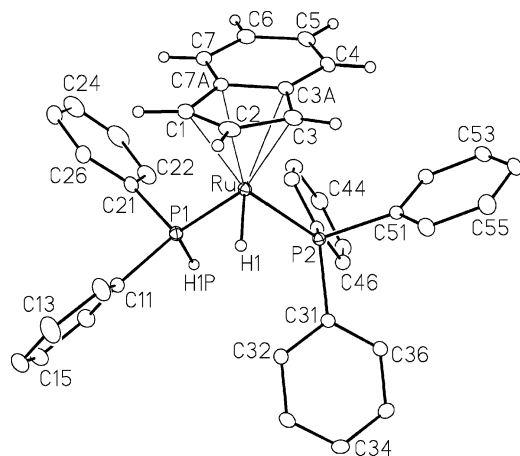**Figure 5.** Molecular structure of [RuH(η^5-indenyl)(HPCy$_2$)(PPh$_3$)] (**5a**).

Figure 6. View of [RuH(η^5-indenyl)(HPPh$_2$)(PPh$_3$)] (**5b**).

Table 4. Selected Interatomic Distances (Å) and Bond and Torsional Angles (deg) in the Structures of [RuH(η^5-indenyl)(HPCy$_2$)(PPh$_3$)] (5a) and [RuH(η^5-indenyl)(HPPh$_2$)(PPh$_3$)] (5b)

	5a	**5b**
	Interatomic Distances	
Ru−P1	2.2736(4)	2.2324(5)
Ru−P2	2.2521(4)	2.2536(5)
Ru−H1	1.53(2)	1.49(2)
Ru−C*^{a}	1.949	1.928
Ru−C7A	2.3948(15)	2.3523(16)
Ru−C1	2.2527(15)	2.2304(17)
Ru−C2	2.2107(15)	2.2117(17)
Ru−C3	2.2388(16)	2.2452(16)
Ru−C3A	2.3816(15)	2.3564(16)
P1−H1P	1.338(18)	1.30(2)
Δ^b	0.15	0.12
	Bond Angles	
C*−Ru−P1^a	130.7	128.7
C*−Ru−P2^a	128.9	130.7
C*−Ru−H1^a	120.9	120.0
P1−Ru−P2	95.680(14)	91.696(15)
P1−Ru−H1	81.2(8)	86.1(8)
P2−Ru−H1	81.0(8)	85.0(8)
fold angle (FA)^c	7.56(10)	6.73(19)
hinge angle (HA)^d	4.89(10)	4.6(2)
	Torsional Angles	
C**−C*−Ru−P1^{a,e}	63.6	−77.7
C**−C*−Ru−P2^{a,e}	−85.9	59.9
C**−C*−Ru−H1^{a,e}	169.8	171.2

^{a} C* = C7A−C1−C2−C3−C3A centroid. ^{b} Δ slip distortion parameter = d(Ru−C7A,C3A) − d(Ru−C1,C3). ^{c} Fold angle = angle between normals to planes defined by C1−C2−C3 and C7A−C3A−C4−C5−C6−C7. ^{d} Hinge angle = angle between normals to planes defined by C1−C2−C3 and C7A−C1−C3−C3A. ^{e} C** = C7A−C3A−C4−C5−C6−C7 centroid.

preferred solution conformation analogous to the solid-state structure (Figure 7). Thus, in solution, the indenyl benzo ring lies preferentially over the space between the dicyclohexylphosphine and PPh$_3$ ligands on the opposite face of the complex. This greatly reduces the interactions between aromatic rings on the indenyl and PPh$_3$ ligands, relative to complex **2a**, which reduces the chemical shift differences and lowers the coalescence temperature for exchange between magnetically inequivalent PPh$_3$ phenyl rings.

The solid-state structure of **5b** (R = Ph) again shows the strongly trans-influencing hydride ligand anti to the
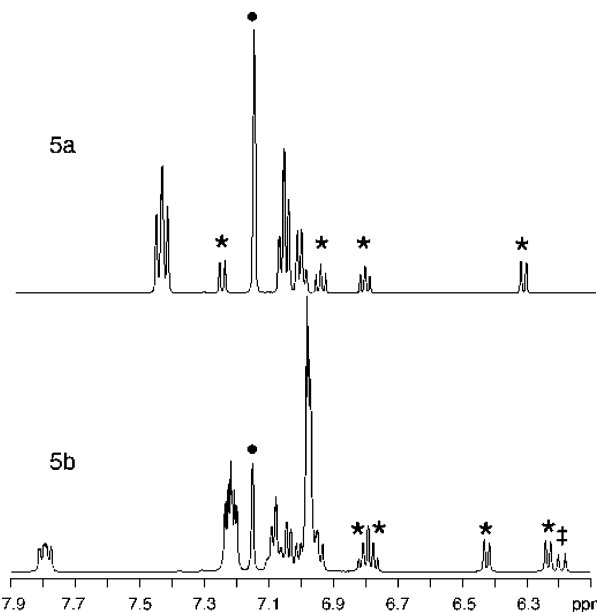
---

(16) We see no evidence for H abstraction from the bound secondary phosphine ligands in these reactions.

Figure 7. Aromatic region of 500 MHz ^{1}H NMR spectra for complexes **5a,b** in C$_6$D$_6$ at room temperature. Peaks due to the η^5-indenyl ligand are marked with asterisks (*), a solid dot (•) indicates the solvent peak C$_5$D$_5$H, and a double dagger (‡) indicates half of the P−H signal in **5b**.

benzo ring of the indenyl ligand. A smaller angle between the two phosphine ligands in this complex leaves the PPh$_3$ ligand closer to the C$_6$ ring than in **5a**.

5a   **5b**
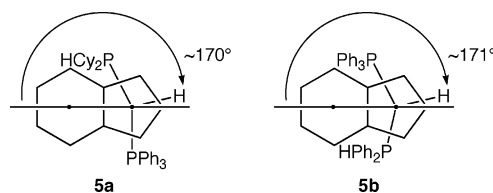
However, the small size of the hydride ligand apparently allows the PPh$_3$ phenyl groups to keep their distance from the indenyl benzo fragment in this complex, and accordingly, the aromatic region of the ^{1}H NMR contains sharper signals than for **2b** (Figures 3 and 7).[17]

The preferred solution conformation dictated by the relative trans influence of piano-stool legs in these mixed-phosphine, half-sandwich Ru complexes may be diagnosed in a general fashion by the apparent symmetry observed for the three PPh$_3$ phenyl groups in low-temperature-limiting spectra. Thus, if the preferred indenyl rotational conformation places the PPh$_3$ ligand within the shielding range of the benzo ring of the indenyl ligand, enhanced chemical shift differences for distinct PPh$_3$ phenyl group signals in ^{1}H and/or ^{13}C NMR spectra are likely to allow observation of slowed rotation around the Ru−PPh$_3$ bond at reasonably accessible temperatures. Variable-temperature NMR data collected for the cationic bis(diethylphosphine) complex [Ru(η^5-indenyl)(HPEt$_2$)$_2$(PPh$_3$)]Cl (**3c**) provide some support for this. Figure 8, which shows the aromatic region of ^{1}H NMR spectra of **3c** recorded at room and low

---

(17) In this context, slight broadening of the PPh$_3$ C$_{ortho}$ signal in the room-temperature 125.7 MHz ^{13}C{^{1}H} NMR spectrum of **5b**, absent in the analogous spectrum of **5a**, provides further evidence that the solid-state structure of **5b** is maintained in solution.
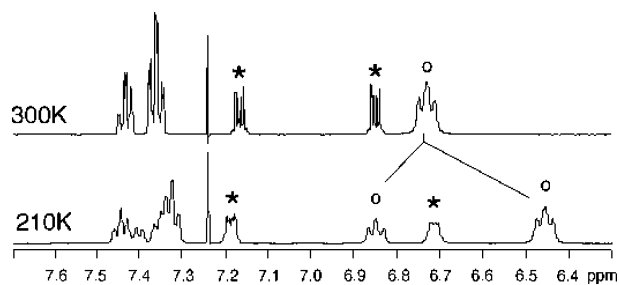
Figure 8. Aromatic region of 360 MHz ^{1}H NMR spectra for complex **3c** in CDCl$_3$ at room temperature and low temperature. Peaks due to the η^5-indenyl ligand are marked with asterisks (*), and "o" indicates signals due to the ortho protons.

temperature, illustrates decoalescence (occurring at ~255 K) of the room-temperature H$_{ortho}$ signal into two peaks of 1:2 intensity separated by approximately 150 Hz at the low-temperature limit. This is consistent with a ground-state structure that places two phenyl rings in a magnetic environment distinct from that of the third phenyl group, the resulting chemical shift difference being enhanced by an approximately gauche conformation of the indenyl benzo ring relative to the PPh$_3$ ligand. This is the conformation one might predict on the basis of the premise that diethylphosphine is a stronger trans-influence ligand than PPh$_3$.

As mentioned in the Introduction, kinetic studies carried out by Gimeno et al. of the substitution of **1** by tertiary phosphines point to a dissociative mechanism in these reactions, rather than an associative mechanism relying on η^5–η^3 indenyl ring slippage.[5] This is attributed to stabilization of the coordinatively unsaturated, 16e intermediate by the η^5-indenyl ligand, a relatively strong donor. We presume a similar mechanism is in effect for the reactions shown in Schemes 1 and 2. However, in contrast to the previously reported tertiary phosphine substitution reactions, in which the second equivalent of incoming phosphine displaces PPh$_3$ to give neutral complexes of the formula [RuCl(η^5-indenyl)(PR$_3$)$_2$],[5] the patterns of substitution we observe suggest that, once a PPh$_3$ ligand at the reasonably sterically crowded Ru in **1** has been substituted by a secondary phosphine, the chloride ligand becomes more labile than the remaining PPh$_3$ ligand, despite its smaller size. We have monitored reactions of **1** with 1–3 equiv and more of secondary phosphines in both polar and nonpolar solvents (toluene, benzene, dichloromethane) but have not observed analogous neutral bis(secondary phosphine) products. The secondary phosphines we have examined are both larger than and comparable in size to PMe$_3$ (cone angle 118°[14]), which was used in earlier studies;[5] thus, it is unlikely that diminished steric crowding prompts preferential displacement of the Cl$^-$ ligand over the remaining PPh$_3$ in complexes **2a**–**c**. Our original presumption (vide supra) that the high trans influence of the secondary phosphines examined here, relative to PPh$_3$, might be due to their increased σ-donor abilities, which could encourage dissociation of the π-donor Cl$^-$ in preference to the reasonably π-accepting PPh$_3$ from an unusually electron-rich Ru center, does not explain why substitutions analogous to ours were not observed for reactions of the strongly σ-donating PMe$_3$ with **1**. Direct compari-

sons of the electronic properties of secondary phosphines with tertiary phosphines are limited;[18] however, Tolman electronic parameters point to a decrease in the *net* donor ability of these three ligands in the order HPCy$_2$ > PPh$_3$ > HPPh$_2$.[19] A decrease in crystallographic and solution ^{13}C{^{1}H} NMR indenyl slippage values (Δ) for **2a**,**b** (see Tables 2 and 3) relative to that for **1**[20] indicates less distortion from η^5 toward η^3 binding of the indenyl ligand to Ru in the mixed-phosphine complexes, a feature which has been considered diagnostic of enhanced π-acceptor properties of the ligand L in the two-legged piano-stool complexes [Rh(η^5-indenyl)L$_2$].[21] Thus, the stronger trans influence of HPR$_2$ relative to PPh$_3$ may be at least partially attributable to increased π acidity of these secondary phosphines relative to PPh$_3$.[22] If this is so, it is difficult to rationalize the observed differences in the order of ligand substitution for reactions of **1** with tertiary or secondary phosphines using simple inductive arguments. Clearly more information is required to assess the impact of the σ- and π-electronic properties of these secondary phosphine ligands on their behavior as ancillary ligands.

Conclusion

Solution and solid-state analysis of the η^5-indenyl conformation in mixed secondary/tertiary phosphine complexes indicates that the secondary phosphines HPCy$_2$ and HPPh$_2$ have a stronger trans influence than PPh$_3$. Further studies are underway to probe the reactivity of **2a**–**c** toward substitution by non-phosphine donors and activation of the P–H bond at the coordinated secondary phosphine in these complexes.

(18) Examples include crystallographic and ^{31}P{^{1}H} NMR studies of *cis*-PtCl$_2$LL′ complexes of dimesitylphosphine and/or triphenylphosphine, indicating comparable electronic (and steric) properties for these two ligands (Pelczar, E. M.; Nytko, E. A.; Zhuravel, M. A.; Smith, J. M.; Glueck, D. S.; Sommer, R.; Incarvito, C. D.; Rheingold, A. L. *Polyhedron* **2002**, *21*, 2409) and measurement of the Tolman electronic parameters[19] for a series of Ni(CO)$_3$L complexes where L = HPRAr* (R = Me, Ph, Ar*; Ar* = 2,4,6-R′$_3$C$_6$H$_2$, R′ = Me, ^{i}Pr, tBu), indicating that the net donor abilities of these bulky secondary phosphines are comparable to or slightly lower than that for PPh$_3$ (Brauer, D. J.; Bitterer, F.; Dörrenbach, Hessler, G.; Stelzer, O.; Krüger, C.; Lutz, F. *Z. Naturforsch.* **1996**, *51b*, 1183).

(19) Tolman electronic parameters (ν_{CO}(A$_1$) values for Ni(CO)$_3$L) represent the net donor properties of the ligands, without distinguishing between σ and π effects. These have been measured for PPh$_3$ (2068.9 cm^{-1}) and HPPh$_2$ (2073.3 cm^{-1}) and may be calculated for HPCy$_2$ (2064.6 cm^{-1}) using Tolman's equation for the additive electronic effects of each substituent. Tolman, C. A. *J. Am. Chem. Soc.* **1970**, *92*, 2953.

(20) The crystallographic slip factor for **1** is 0.21 Å (Kamigaito, M.; Watanabe, Y.; Ando, T.; Sawamoto, M. *J. Am. Chem. Soc.* **2002**, *124*, 9994). The slip factor for **1** in solution, determined by ^{13}C{^{1}H} NMR (see Table 2), is $\Delta\delta$(C$_{3a,7a}$) = δ(C$_{3a,7a}$(**1**)) − δ(C$_{3a,7a}$(η-sodium indenyl)) = 111.5 ppm − 130.7 ppm = −19.2 ppm.

(21) Marder, T. B.; Calabrese, J. C.; Roe, D. C.; Tulip, T. H. *Organometallics* **1987**, *6*, 2012. The magnitude of slip factor variation from **1** to **2a**,**b** (0.06 Å) is comparable to that cited by Marder et al. as diagnostic of very different ligand donor/acceptor properties within the Rh(I) systems, although we are not certain that such a straightforward electronic analysis is as reliable for the more sterically congested Ru(II) systems.

(22) Support for the proposed increase in π acidity of HPR$_2$ relative to PPh$_3$ comes from evaluation by Emsley of three factors relevant to the strength of metal–phosphine complexation (σ-bond strength, π-bond strength, and steric bulk). This analysis suggests that PH$_3$ should form stronger M–L bonds than most PR$_3$ (including PPh$_3$) and highlights the likely comparable σ-donor ability, greater π-acceptor ability, and (typically) smaller size of HPR$_2$ relative to PPh$_3$. Emsley, J. *The Chemistry of Phosphorus*; Harper and Row: New York, 1976; p 203.

Experimental Section

General Comments. Unless otherwise noted, all reactions and manipulations were performed under nitrogen in an MBraun Unilab 1200/780 glovebox or using conventional Schlenk techniques. Toluene was dried by distillation from sodium under argon; benzene, pentane, hexanes, tetrahydrofuran, and ether were distilled from sodium/benzophenone under argon; methylene chloride was dried by distillation from P_2O_5 under argon. Deuterated solvents were purchased from Canadian Isotope Labs (CIL), freeze−pump−thaw degassed, and vacuum transferred from sodium/benzophenone (benzene-d_6, toluene-d_8) or calcium hydride (chloroform-d) before use. Diphenyl-, dicyclohexyl-, and diethylphosphine were purchased from Strem Chemicals as 10 wt % solutions in hexanes, and the concentrations were checked against a known quantity of triphenylphosphine oxide by $^{31}P\{^1H\}$ NMR before use. [RuCl-(η^5-indenyl)(PPh$_3$)$_2$] (**1**) was prepared using the literature method.[23] NMR spectra were acquired on a Bruker AC 300 operating at 300.133 MHz for ^1H and 75.469 MHz for ^{13}C, a Bruker AMX 360 operating at 360.13 MHz for ^1H, 90.565 MHz for ^{13}C, 145.784 MHz for ^{31}P, and 71.550 MHz for ^{29}Si, and a Bruker Avance 500 operating at 500.133 MHz for ^1H, 202.430 MHz for ^{31}P, and 99.361 MHz for ^{29}Si. Chemical shifts are reported in ppm at ambient temperature unless otherwise stated. ^1H chemical shifts are referenced to residual protonated solvent peaks at 7.16 ppm (C$_6$D$_5$H), 2.09 ppm (PhCD$_2$H), and 7.24 ppm (CHCl$_3$). ^{13}C chemical shifts are referenced to C$_6$D$_6$ at 128.4 ppm and CDCl$_3$ at 77.5 ppm. ^1H, ^{13}C, and ^{29}Si chemical shifts are reported relative to tetramethylsilane, and ^{31}P chemical shifts are reported relative to 85% H$_3$PO$_4$(aq). Melting/decomposition temperatures, recorded using a Gallenkamp apparatus for capillary samples, are uncorrected for ambient pressure. Microanalysis was performed by Canadian Microanalytical Service Ltd., Delta, BC, Canada. (Note: the chloride-containing complexes **2a,b** and **3c** gave % C analyses slightly outside the ±0.4% range; thus, we have included ^1H NMR spectra of these compounds in the Supporting Information to illustrate their purities.) IR spectra were recorded on a Perkin-Elmer FTIR Spectrum 1000 spectrophotometer using KBr pellets. Mass spectrometry was carried out by Mr. David McGillivray at the Department of Chemistry, University of Victoria.

Synthesis of [RuCl(η^5-indenyl)(HPCy$_2$)(PPh$_3$)] (2a). To a Schlenk flask containing a dark red solution of [RuCl-(indenyl)(PPh$_3$)$_2$] (**1**; 1.413 g, 1.820 mmol) in CH$_2$Cl$_2$ (20 mL) was added a 0.7 M hexanes solution of HPCy$_2$ (6.1 mL, 4 mmol, 2.2 equiv). A condenser was attached to the top of the Schlenk flask, and the solution was stirred and refluxed for a total of 6 h. The progress of the reaction was monitored by $^{31}P\{^1H\}$ NMR, through the periodic withdrawal of 0.15 mL aliquots of the reaction mixture. The red color of the solution lightened slightly during the reaction. After the reaction mixture had cooled, the CH$_2$Cl$_2$/hexanes was removed by evaporation, and toluene (9 mL) was added to the residue, producing a fine orange precipitate and light red supernatant liquid. The orange powder was isolated by cannula filtration, redissolved in a minimum volume of CH$_2$Cl$_2$, and crystallized using slow diffusion of hexanes. Two crops of red crystals gave a total yield of 0.890 g, 69%. The first crop (0.438 g, 34%) was used for microanalysis.

$^{31}P\{^1H\}$ NMR (200.5 MHz, CDCl$_3$, δ): 68.3 (d, $^2J_{PP}$ = 42 Hz, H*P*(C$_6$H$_{11}$)$_2$), 50.7 (d, *P*Ph$_3$). Anal. Calcd for C$_{39}$H$_{45}$ClP$_2$Ru: C, 65.77; H, 6.37. Found: C, 65.28; H, 6.40. IR: 2319 cm^{-1} (m, ν_{P-H}, surrounded by some fine structure). MS (+LSIMS, matrix mNBA; *m/z* (relative intensity)): 712 (100%) [M$^+$]; 677 (90%) [M − Cl]; 613 (45%) [mNBA]; 596 (15%) [M − indenyl]; 559 (12) [M − indenyl, Cl]; 514 (40) [M − HPCy$_2$]; 479 (90) [M − Cl, HPCy$_2$].

Synthesis of [RuCl(η^5-indenyl)(HPPh$_2$)(PPh$_3$)] (2b). To a Schlenk flask containing a dark red solution of [RuCl-(indenyl)(PPh$_3$)$_2$] (**1**; 1.5 g, 1.9 mmol) in CH$_2$Cl$_2$ (20 mL) was added a 0.395 M hexanes solution of HPPh$_2$ (10 mL, 3.9 mmol, 2.1 equiv). A condenser was attached to the top of the Schlenk flask, and the solution was stirred and refluxed for 2 h. (The progress of the reaction was monitored by $^{31}P\{^1H\}$ NMR, through the periodic withdrawal of 0.2 mL aliquots of the reaction mixture.) After the reaction mixture had cooled, the CH$_2$Cl$_2$/hexanes was removed under vacuum, and the flask was taken into the glovebox. Trituration of the residual dark red oil with hexanes (4 × 20 mL) gave a powdery, bright orange precipitate, which was isolated by filtration. Yield: 1.13 g (1.61 mmol, 84.7%). A 0.192 g portion of the product was recrystallized by slow diffusion of hexanes into a concentrated CH$_2$Cl$_2$ solution, which gave red crystals (0.133 mg) used for microanalysis.

$^{31}P\{^1H\}$ NMR (145.8 MHz, CDCl$_3$), 50.7 (d, $^2J_{PP}$ = 49 Hz, H*P*(C$_6$H$_5$)$_2$), 47.36 (d, *P*(C$_6$H$_5$)$_3$). Anal. Calcd for C$_{39}$H$_{33}$-ClP$_2$Ru: C, 66.90; H, 4.75. Found: C, 66.14; H, 4.97. MS (+LSIMS, matrix mNBA; *m/z* (relative intensity)): 700 (77%) [M$^+$]; 665, (50%) [M − Cl]; 514, (55%) [M − PPh$_3$]; 479, (100%) [M − Cl, HPPh$_2$]; 402, (57%), [M − Cl, PPh$_3$]. IR: 2339 (m, ν_{P-H}). Dec pt: 200 °C.

Synthesis of [RuCl(η^5-indenyl)(HPEt$_2$)(PPh$_3$)] (2c). To a Schlenk flask containing a dark red solution of [RuCl-(indenyl)(PPh$_3$)$_2$] (**1**; 1.5 g,1.9 mmol) in CH$_2$Cl$_2$ (15 mL) was added a 0.6 M hexanes solution of HPEt$_2$ (3.0 mL, 2 mmol, 1.1 equiv). A condenser was attached to the top of the Schlenk flask, and the solution was stirred and refluxed for 2 h. The red color of the solution lightened slightly during the reaction, which was shown to be complete by $^{31}P\{^1H\}$ NMR of a 0.1 mL aliquot in CDCl$_3$. After the reaction mixture had cooled, the CH$_2$Cl$_2$/hexanes was removed by evaporation, and the resulting red residue was triturated and then washed with hexanes (100 mL total), giving an orange powder, which was isolated by filtration. Crude yield: 1.08 g (1.8 mmol, 94%). A 0.200 g portion of this crude product, which contained some **3c** and an unidentified impurity ($^{31}P\{^1H\}$ in CDCl$_3$: 42.7 (d, $^2J_{PP} \approx$ 17−18 Hz) and 2.9 (t)),[24] was redissolved in a minimum volume of benzene and crystallized using slow diffusion of hexanes. The resulting red crystals (0.117 g, 55% cumulative yield) still contained a small amount of the unidentified contaminant (see the Supporting Information for NMR spectra) and so were not submitted for microanalysis. (This recrystallization was tried repeatedly on reasonably clean crude samples, with similar results.)

$^{31}P\{^1H\}$ NMR (200.5 MHz, CDCl$_3$, δ): 53.4 (d, $^2J_{PP}$ = 49 Hz, *P*Ph$_3$), 46.28 (d, H*P*Et$_2$); HR-MS (FAB, matrix mNBA): exact mass (monoisotopic) calcd for C$_{31}$H$_{33}$ClP$_2$Ru, 604.0790; found, 604.0799 ± 0.0002 (average of three trials). IR (crude product): 2295 cm^{-1} (m, broad, ν_{P-H}).

Synthesis of [Ru(η^5-indenyl)(HPEt$_2$)$_2$(PPh$_3$)]Cl (3c). To a Schlenk flask containing a dark red solution of [RuCl-(indenyl)(PPh$_3$)$_2$] (**1**; 1.5 g, 1.9 mmol) in CH$_2$Cl$_2$ (15 mL) was added a 0.7 M hexanes solution of HPEt$_2$ (5.4 mL, 3.8 mmol, 2.0 equiv) via syringe, under nitrogen. The resulting mixture (still red) was stirred at room temperature, and the progress of the reaction was monitored by the periodic withdrawal of aliquots for $^{31}P\{^1H\}$ NMR analysis. After 36 h the solvent was removed under vacuum, giving a red-orange residue, which was washed with hexanes (100 mL) and filtered, to give a yellow-orange powder comprised of the desired complex **3c**, the monosubstituted [RuCl(η^5-indenyl)(HPEt**$_2$**)(PPh$_3$)] (**2c**),

(23) Oro, L. A.; Ciriano, M. A.; Campo, M. *J. Organomet. Chem.* **1985**, *289*, 117.

(24) This unknown species may arise from the Ru coordination of small amounts of Et$_2$POH present in the standard hexanes solution of HPEt$_2$ used in this synthesis. The coordination of tautomeric secondary phosphine oxides at "η^5-Cp′Ru" has been probed via the deliberate addition of oxygen to diphenylphosphine complexes of this fragment: Torres-Lubián, R.; Rosales-Hoz, M. J.; Arif, A. M.; Ernst, R. D.; Paz-Sandoval, M. A. *J. Organomet. Chem.* **1999**, *585*, 68.

Table 5. Crystallographic Experimental Details

	2a	2b	5a	5b
formula	$C_{39}H_{45}ClP_2Ru$	$C_{39}H_{33}ClP_2Ru$	$C_{39}H_{46}P_2Ru$	$C_{39}H_{34}P_2Ru$
fw	712.21	700.11	677.77	665.67
cryst size (mm)	$0.23 \times 0.16 \times 0.11$	$0.26 \times 0.16 \times 0.08$	$0.73 \times 0.50 \times 0.32$	$0.39 \times 0.35 \times 0.26$
cryst syst	monoclinic	monoclinic	monoclinic	monoclinic
space group	$P2_1/n^a$	$P2_1/c$ (No. 14)	$P2_1/c$ (No. 14)	$P2_1/c$ (No. 14)
a (Å)	10.0703(6)	13.7599(8)	20.8844(9)	9.8422(9)
b (Å)	18.1219(11)	11.3513(6)	8.6214(4)	17.8223(17)
c (Å)	18.3053(11)	21.8632(12)	19.8587(9)	18.2126(17)
β (deg)	95.4228(12)	107.7164(10)	112.1293(7)	103.0787(14)
V (Å^3)	3325.6(3)	3252.9(3)	3312.2(3)	3111.8(5)
Z	4	4	4	4
ρ_{calcd} (g cm^{-3})	1.422	1.430	1.359	1.421
μ (mm^{-1})	0.675	0.689	0.596	0.634
temp (°C)	-80	-80	-80	-80
max 2θ (deg)	52.82	52.80	52.76	52.74
total no. of data collected	23 559	22 560	24 112	23 722
no. of unique data, R_{int}	6806, 0.0639	6655, 0.0412	6766, 0.0171	6360, 0.0248
no. of obsd data ($I \geq 2\sigma(I)$)	5283	5448	6461	5747
no. of restraints/params	0/392	0/392	0/387	0/387
$S(F^2)$ (all data)^b	1.070	1.094	1.064	1.034
$R_1(F)$ ($I \geq 2\sigma(I)$)^c	0.0478	0.0391	0.0208	0.0229
$wR_2(F^2)$ (all data)^c	0.1188	0.1060	0.0555	0.0626
$\Delta_{\sigma max}, \Delta_{\sigma min}$ (e Å^{-3})	2.097, -0.471	2.019, -0.364	0.481, -0.341	0.488, -0.225

^{a} An alternate setting of $P2_1/c$ (No. 14). ^{b} $S = [\sum w(F_o^2 - F_c^2)^2/(n - p)]^{1/2}$ (n = number of data; p = number of parameters varied; $w = [\sigma^2(F_o^2) + (a_0P)^2 + a_1P]^{-1}$, where $P = [\text{Max}(F_o^2, 0) + 2F_c^2]/3$; for **2a**, $a_0 = 0.0634$, $a_1 = 0.6216$; for **2b**, $a_0 = 0.0519$, $a_1 = 2.8872$; for **5a**, $a_0 = 0.0255$, $a_1 = 2.0065$; for **5b**, $a_0 = 0.0345$, $a_1 = 1.1923$). ^{c} R1 $= \sum||F_o| - |F_c||/\sum|F_o|$; wR2 $= [\sum w(F_o^2 - F_c^2)^2/\sum w(F_o^4)]^{1/2}$.

and a trace of an impurity (^{31}P{^{1}H} NMR in CDCl$_3$: δ 30.2 (s)) tentatively assigned to the trisubstituted cation [Ru(η^5-indenyl)(HPEt$_2$)$_3$]Cl (**4c**). Washing with benzene (50 mL) gave the product **3c** as a bright yellow powder, still with a trace (<5%) of **4c**. Yield: 0.055 g, 0.79 mmol, 41%. (The red benzene washings yielded $\sim$0.165 g of **2c**, after trituration with CH$_2$Cl$_2$.) Recrystallization of 0.154 g of crude **3c** from CH$_2$Cl$_2$ (1 mL) layered with hexanes (4 mL) gave dark yellow crystals. These were finely ground and washed with hexanes to yield 0.140 g of a yellow microcrystalline powder, which was used for elemental analysis and high-resolution MS.

^{31}P{^{1}H} NMR (200.5 MHz, CDCl$_3$, δ): 51.6 (t, $^2J_{PP}$ = 35 Hz, PPh$_3$), 34.5 (d, HP(C$_2$H$_5$)$_2$). Anal. Calcd for C$_{35}$H$_{44}$ClP$_3$Ru: C, 60.56; H, 6.39. Found: C, 60.12; H, 6.39. MS (+LSIMS, matrix mNBA; m/z (relative intensity)): 659 (100%) [M − Cl]; 569 (28%) [M − Cl, HPEt$_2$]; 479 (33%) [M − Cl, 2HPEt$_2$]; 397 (51%) [M − Cl, PPh$_3$]. HR-MS (FAB, matrix mNBA): exact mass (monoisotopic) calcd for M − Cl, 659.1699; found, 659.1702 ± 0.0005 (average three trials). IR: 2314 cm^{-1} (w, ν_{P-H}).

Synthesis of [Ru(η^5-indenyl)(HPCy$_2$)$_3$]Cl (4a). The following preparation gave mixtures of **2a** and **4a**, from which **4a** was isolated cleanly enough for spectroscopic characterization. A 0.5 M hexanes solution of PCy$_2$H (5.1 mL, 2.6 mmol, 4.3 equiv) was added to a solution of [RuCl(indenyl)(PPh$_3$)$_2$] (**1**; 0.50 g, 0.60 mmol) in toluene (30 mL). This solution was refluxed for 2 h and then cooled to -20 °C, which allowed isolation of three separate crops of orange (**2a**) to yellow (**4a**) powder. The third crop, collected on a filter frit and washed with hexanes (3 × 10 mL), was **4a**. Yield: 0.121 g (26%) of a yellow powder.

^{31}P{^{1}H} NMR (121.5 MHz, CDCl$_3$, δ): 34.3 (s, HPCy$_2$). ^{1}H NMR (300 MHz, CDCl$_3$, δ): 7.42−7.37 (m, 2H, $H_{5,6}$), 7.30−7.25 (m, 2H, $H_{4,7}$), 5.51 (t, $^3J_{HH}$ = 2.6 Hz, 1H, H_2), 5.30 (d, 2H, $H_{1,3}$), 4.78 (dm, $^1J_{PH}$ = 349 Hz, 3H, P−H).

Synthesis of [RuH(η^5-indenyl)(HPCy$_2$)(PPh$_3$)] (5a). To a Schlenk flask containing a red-orange suspension of [RuCl-(η^5-indenyl)(HPCy$_2$)(PPh$_3$)] (**2a**; 0.106 g, 0.149 mmol) in dry MeOH (10 mL) was added a 0.054 M methanol solution of NaOMe (3.4 mL, 0.19 mmol, 1.1 equiv). There was no immediate color change, but after the mixture had been stirred at room temperature for 2 days, a yellow precipitate had formed, which was filtered and washed with dry MeOH (2 × 10 mL) and hexanes (2 × 20 mL) and then dried under vacuum.

Yield: 0.77 mg (76%) of a yellow powder. Anal. Calcd for C$_{39}$H$_{46}$P$_2$Ru: C, 69.04; H, 6.70. Found: C, 69.13; H, 6.80. ^{31}P{^{1}H} NMR (145.78 MHz, C$_6$D$_6$, δ): 70.5 (d, J_{P-P} = 27 Hz, PPh$_3$), 61.3 (d, HP(C$_6$H$_{11}$)$_2$). MS (+LSIMS, matrix mNBA; m/z (relative intensity)): 677 (100%) [M$^+$]; 479 (71%) [M − HPCy$_2$]; 413 (31%) [M − PPh$_3$]; 363 (23%) [M − HPCy$_2$, indenyl]. IR: 2275 (m, ν_{P-H}), 2009 cm^{-1} (m, ν_{Ru-H}). Dec pt: 114−117 °C.

Synthesis of [RuH(η^5-indenyl)(HPPh$_2$)(PPh$_3$)] (5b). This complex was prepared as described above for complex **5a**, using **2b** (239 mg, 0.359 mmol) and a 0.072 M methanol solution of NaOMe (4.7 mL, 0.44 mmol). The mixture was stirred for 4 days instead of 2 days. Yield: 0.175 mg of a yellow powder (77%). Anal. Calcd for C$_{39}$H$_{34}$P$_2$Ru: C, 70.30; H, 5.01; Found: C, 70.29; H, 5.19. ^{31}P{^{1}H} NMR (145.78 MHz, δ): 70.3 (d, J_{P-P} = 33 Hz, PPh$_3$), 49.0 (d, Hz, HPPh$_2$). MS (+LSIMS, matrix mNBA; m/z (relative intensity)): 665 (70%) [M$^+$]; 479 (100%) [M − HPPh$_2$]; 402 (32%) [M − PPh$_3$]. IR: 2262 (m, ν_{P-H}), 2024 cm^{-1} (m, ν_{Ru-H}). Dec pt: 127 °C.

Monitoring the Reaction of [RuCl(η^5-indenyl)(PPh$_3$)$_2$] (1) with a Deficiency of HPEt$_2$ by ^{31}P{^{1}H} NMR Spectroscopy. Compound **1** (30 mg, 0.039 mmol) and the appropriate amount of a 10% hexanes solution of HPEt$_2$ were weighed into a sealable NMR tube in the glovebox. Triphenylphosphine oxide (O=PPh$_3$, 15 mg, 0.054 mmol) was added as an internal standard. The tube was attached to a needle valve adaptor and brought out to the Schlenk line, where CDCl$_3$ (0.5 mL) was added by vacuum transfer. The mixture was degassed using three freeze−pump−thaw cycles, and the tube was flame-sealed and warmed to room temperature. The progress of the reactions was monitored by ^{31}P{^{1}H} NMR spectroscopy using delay times of D1 = 5 s. Product distributions (complexes **1**, **2c**, **3c**, and **4c**) were determined relative to the O=PPh$_3$ internal standards. An initial spectrum indicated the presence of 0.4 equiv of HPEt$_2$, relative to **1**, in this sample.

Line-Shape Analysis for 2a. Line-shape analysis was carried out on the aromatic region of ^{13}C{^{1}H} NMR (125.7 MHz) spectra recorded for compound **2a** in chloroform-d_3 at 280, 260, 250, 240, 230, and 220 K, using gNMR.[25] Rate constants (k) for the three-site exchange were determined iteratively at each temperature, giving well-matched simulated

(25) Budzelaar, P. H. M. gNMR version 3.6.5; Cherwell Scientific Publishing: Palo Alto, CA, 1992−1996.

and experimental spectra (see the Supporting Information). Estimated errors in k varied from 2 to 6%, and temperatures are ± 2 K. The energy of activation, $E_a = 9.1$ kcal/mol, was determined from the slope of an Arrhenius plot ($\ln k$ vs $1/T$, $R^2 = 0.9763$).

X-ray Crystallographic Studies. Single crystals suitable for X-ray diffraction were grown from CH_2Cl_2/hexanes (**2a,b**) or toluene/hexanes (**5a,b**) solutions at -20 °C under nitrogen and mounted on glass fibers in hydrocarbon oil. Selected crystal data and structural refinement details are listed in Table 5; further details are given in the Supporting Information.

Supporting Information Available: Complete X-ray crystallographic information files (CIF) for complexes **2a,b** and **5a,b**, and figures giving ^{1}H NMR spectra for **2a,b** and **3c**, ^{31}P{^{1}H} and ^{1}H NMR spectra for **2c**, and representative low-temperature, simulated, and 2D NMR data for complexes **2a–c**. This material is available free of charge via the Internet at http://pubs.acs.org.

OM050259W